JACS
JOURNAL OF THE AMERICAN CHEMICAL SOCIETY

Article

pubs.acs.org/JACS

OGlcNAcylation and Phosphorylation Have Opposing Structural Effects in tau: Phosphothreonine Induces Particular Conformational Order

Michael A. Brister,[†] Anil K. Pandey,[†] Agata A. Bielska, and Neal J. Zondlo*

Department of Chemistry and Biochemistry, University of Delaware, Newark, Delaware 19716, United States

Supporting Information

ABSTRACT: Phosphorylation and OGlcNAcylation are dynamic intracellular protein post-translational modifications that frequently are alternatively observed on the same serine and threonine residues. Phosphorylation and OGlcNAcylation commonly occur in natively disordered regions of proteins, and often have opposing functional effects. In the microtubule-associated protein tau, hyperphosphorylation is associated with protein misfolding and aggregation as the neurofibrillary tangles of Alzheimer's disease, whereas OGlcNAcylation stabilizes the soluble form of tau. A series of peptides derived from the proline-rich domain (residues 174−251) of tau was synthesized, with free Ser/Thr hydroxyls, phosphorylated Ser/Thr (pSer/pThr), OGlcNAcylated Ser/Thr, and diethylphosphorylated Ser/Thr. Phosphorylation and OGlcNAcylation were found by CD and NMR to have opposing structural effects on polyproline helix (PPII) formation, with phosphorylation favoring PPII, OGlcNAcylation opposing PPII, and the free hydroxyls intermediate in structure, and with phosphorylation structural effects greater than OGlcNAcylation. For $tau_{196–209}$, phosphorylation and OGlcNAcylation had similar structural effects, opposing a nascent α-helix. Phosphomimic Glu exhibited PPII-favoring structural effects. Structural changes due to Thr phosphorylation were greater than those of Ser phosphorylation or Glu, with particular conformational restriction as the dianion, with mean $^3J_{\alpha N}$ = 3.5 Hz (pThr) versus 5.4 Hz (pSer), compared to 7.2, 6.8, and 6.2 Hz for Thr, Ser, and Glu, respectively, values that correlate with the backbone torsion angle ϕ. Dianionic phosphothreonine induced strong phosphothreonine amide protection and downfield amide chemical shifts (δ_{mean} = 9.63 ppm), consistent with formation of a stable phosphate-amide hydrogen bond. These data suggest potentially greater structural importance of threonine phosphorylation than serine phosphorylation due to larger induced structural effects.

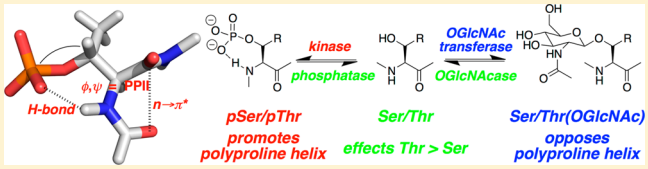

INTRODUCTION

Genome sequencing has revealed that most higher eukaryotes have a relatively limited set of genes, whose numbers do not correlate with organismal complexity.[1] The ability of a limited number of genes to achieve diverse protein functions depends on a series of post-translational modifications (PTMs), including phosphorylation, glycosylation, acylation, methylation, lipidation, protein ligation, sulfation, and myriad oxidations, that result in controllable and conditional functions of proteins. Intracellularly, serine and threonine residues are modified by phosphorylation, regulated by protein kinases and phosphatases that collectively account for 2.5% of human genes, and by OGlcNAcylation, controlled by OGlcNAc transferases and OGlcNAcases (Figure 1).[2] Frequently, the same residues that are phosphorylated are also observed under different conditions to be OGlcNAcylated. Interestingly, in many cases, phosphorylation and OGlcNAcylation are observed to have opposing functional effects. Thus, improved understanding of the differential structural effects of phosphorylation and OGlcNAcylation is of broad potential application in cellular biology.

The protein tau is a 441 amino acid (largest isoform) natively disordered microtubule-binding protein that is most prominent in neurons. Hyperphosphorylated forms of tau aggregate as fibrils and precipitate as the major protein components of the neurofibrillary tangles (NFTs) observed in Alzheimer's disease and other neurodegenerative disorders, including frontotemporal dementia, Pick's disease, and chronic traumatic

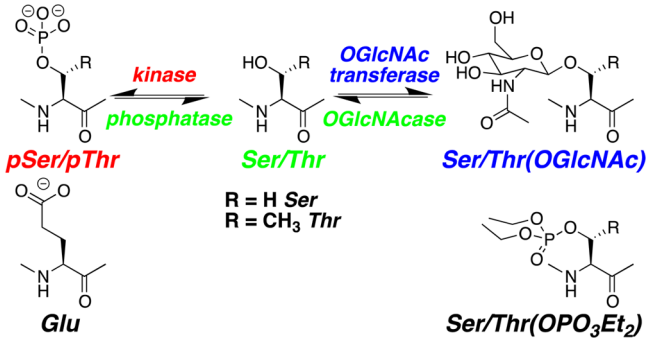

Figure 1. Intracellular post-translational modifications of Ser and Thr by phosphorylation and OGlcNAcylation. Glu is a common pSer/pThr mimic. The diethylphosphate triester of Ser/Thr is neutral and sterically similar to OGlcNAc.

Received: July 12, 2013
Published: February 21, 2014

   dx.doi.org/10.1021/ja407156m | J. Am. Chem. Soc. 2014, 136, 3803−3816

encephalopathy (CTE) (collectively termed tauopathies).[3] The protein tau consists of a number of functional domains (Figure 2), including 4 hydrophobic tubulin-binding domains (TBDs)

$tau_{174-183}$ $K_{174}TPPAPKTPP_{183}$
$tau_{196-209}$ $G_{196}YSSPGSPGTPGSR_{209}$
$tau_{211-219}$ $YR_{211}TPSLPTPP_{219}$
$tau_{229-238}$ $YV_{229}RTPPKSPSS_{238}$

$tau_{211-238}$ $R_{211}TPSLPTPPTREPKKVAVVRTPPKSPSS_{238}$
$tau_{234-251}$ $K_{234}SPSSAKSRLQTAPVPMP_{251}$

Figure 2. Top: Schematic of the primary sequence and functional domains of tau. Red, hydrophobic regions A and B; green, proline-rich domain (PRD); blue, tubulin-binding domain (TBD) repeats 1−4 (R1, R2, R3, R4). The most commonly used boundaries of the TBDs are indicated; notably, residues 242−251 of R1 have poor homology to analogous residues in R2, R3, and R4 thus defined. The TBD boundaries have alternatively been defined as R1 residues 252−282, R2 283−313, R3 314−344, R4 345−376. By this definition, the proline-rich domain extends through proline 251. Most phosphorylation sites associated with tau aggregation in Alzheimer's disease are in the proline-rich domain and in the C-terminal domain. Additional phosphorylation sites are in the N-terminus and in the TBDs. Bottom: Sequences of tau-derived proline-rich peptides examined in this study. All peptides were acetylated at the N-terminus and contained C-terminal amides. Residues in blue indicate sites modified by phosphorylation, diethylphosphorylation, or OGlcNAcylation. Residues in red correspond to the key residues of the hydrophobic B motif. Residue numbers are based on the largest (441 residue) isoform of tau. N-terminal tyrosines were added to $tau_{211-219}$ and $tau_{229-238}$ for concentration determination. In contrast to these peptides, addition of either an N-terminal or C-terminal Tyr to $tau_{174-183}$ resulted in substantial changes to its CD spectrum.

(residues 242−367) that are directly responsible for both binding microtubules and for tau aggregation, an N-terminal hydrophobic region which dynamically interacts with the TBDs, and a proline-rich domain (residues 174−241), which also contains a second hydrophobic region (residues 220−231).[4] The proline-rich domain of tau serves as a linker between the N-terminal sequence and the tubulin-binding domains. The majority of phosphorylation sites identified to be important to hyperphosphorylation-mediated tau aggregation are in the proline-rich domain, with additional phosphorylation sites located C-terminal to the tubulin-binding domains in a region that also interacts with the TBD to stabilize it.

Knowledge of the structural effects of post-translational modifications of tau is important to understand the mechanisms of pathological protein misfolding induced by hyperphosphorylation observed in the Alzheimer's diseased brain, as well as to understand how to maintain tau in a soluble, nonaggregated form. Data on natively disordered proteins, including tau, indicate that conformations observed in peptides are similar to those observed in the larger protein contexts, because of the absence of stable tertiary and quaternary structures.[5] Because of the challenges of both structure determination in natively disordered proteins and of reliable preparation of homogeneous samples of expressed proteins with defined patterns of multiple protein post-translational modifications, particularly for OGlcNAcylation, we have used peptide models to understand the local structural effects of natively disordered regions of proteins.[6]

We previously investigated the structural effects of phosphorylation on peptides derived from the proline-rich domain of tau.[7] In that work, we found that phosphorylation of tau peptides induced a structural change promoting polyproline helix (PPII). OGlcNAcylation of tau, which has been identified on a series of sites in the proline-rich domain that are also sites of phosphorylation, has been found to be protective against hyperphosphorylation and neurofibrillary tangle formation.[8] Indeed, inhibitors of OGlcNAcase, the enzyme that removes the OGlcNAc group and thus can functionally inhibit phosphorylation by preventing access of the kinase substrate, are under investigation as potential therapeutics in Alzheimer's disease.[9] The mechanism of OGlcNAcylation-mediated protection against NFT formation could be via prevention of phosphorylation, and additionally or alternatively OGlcNAcylation could promote a structure change that is different than that of phosphorylation.

RESULTS

In view of the general observation of phosphorylation and OGlcNAcylation occurring on similar sites, particularly within natively disordered regions of proteins, we sought to examine within a biologically relevant sequence context the relative structural effects of phosphorylation and OGlcNAcylation compared to the unmodified Ser/Thr residues. A series of peptides derived from the proline-rich domain of tau was synthesized, and their structures were analyzed as free hydroxyls and as phosphorylated and OGlcNAcylated amino acids, by circular dichroism and NMR (Figure 2). All residues that contained post-translational modifications have been previously identified as sites of these post-translational modifications in tau.[8,10]

The protected Fmoc β-OGlcNAc serine and threonine amino acids were synthesized via a modification of the methodology of Arsequell et al. (Scheme 1).[11] The protected OGlcNAcylated amino acids were incorporated in peptides, and the peptides were subjected to TFA cleavage/deprotection and purified by HPLC. The purified peptides containing protected OGlcNAc hydroxyls were then subjected to deesterification via NaOMe/MeOH and purified to generate peptides with defined patterns of OGlcNAcylation on multiple residues (Scheme 2).[12]

Scheme 1. Synthesis of OGlcNAcylated Fmoc Amino Acids via a Modification of Ref 11

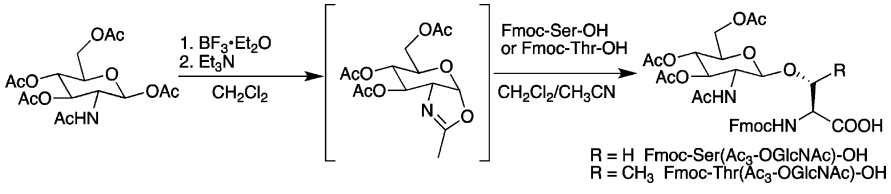

dx.doi.org/10.1021/ja407156m | J. Am. Chem. Soc. 2014, 136, 3803−3816

Scheme 2. Synthesis of OGlcNAcylated Peptides via Initial Purification of the Peracetylated Peptides Followed by Deacetylation under Basic Conditions

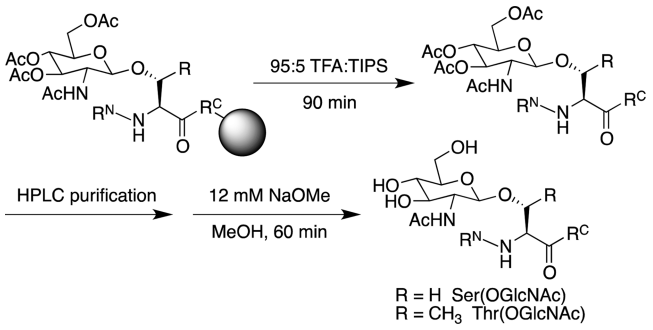

In contrast to the common use of Glu as a mimic of phosphoserine/phosphothreonine, there is no readily accessible mimic of OGlcNAcylated serine/threonine. The diethylphosphate modification of serine and threonine, which is readily incorporated into peptides using phosphoramidites by standard chemistry employed for peptide phosphorylation, generates a derivatized side chain that is neutral and sterically similar to OGlcNAc. However, in contrast to OGlcNAcylated Ser/Thr, which typically require expensive amino acids (Fmoc-Ac_3–SerOGlcNAc and Fmoc-Ac_3–ThrOGlcNAc cost $600/100 mg, a quantity sufficient for the incorporation of just one OGlcNAcylated residue in a single peptide synthesized at small scale) and/or substantial synthetic manipulation, peptides with the diethylphosphate modification are readily synthesized on solid phase from inexpensive, commercially available reagents (Figure 1). Diethylphosphate, which exhibits substantial steric effects in model peptides,[13] is thus potentially a practical mimic of the steric effects of OGlcNAcylation. Therefore, in addition to synthesizing the OGlcNAcylated peptides, we also synthesized peptides with the diethylphosphates at sites of OGlcNAcylation to investigate them as potential readily accessible mimics of OGlcNAcylation.

Polyproline helix (PPII) is a predicted major conformation of protein proline-rich domains.[14] The PPII content in peptides can be quantified using circular dichroism (CD), via the weak positive band at ~228 nm.[15] In larger peptides, the intensity of this band can be obscured by the substantially more intense signal from α-helices ($[\theta]_{max} \sim -33\,000$ deg cm^2 dmol^{-1} for α-helix, compared to $[\theta]_{max} = +5000$ deg cm^2 dmol^{-1} for polyproline helix); thus, even nascent α-helices and β-structure can substantially obscure the CD signal of polyproline helix in larger peptides. PPII is also characterized by a negative band at ~200 nm, although other structures can contribute to the intensity of this band, and thus analysis of this band is nonquantitative. Polyproline helix can also be identified by changes in the λ_{max} in CD and in NMR via coupling constants.[16] In general, it is difficult to identify polyproline helix in larger peptides and proteins by either CD or NMR because of similarities to data in random coil, though polyproline helix can be definitively identified and is observed to thermally melt to a random coil conformation, which has a different CD signature. Because of these complications, smaller peptides often have substantial advantages for the definitive identification of polyproline helix.

In polyproline helix propensity scales, serine and threonine have low PPII propensities, due to the possibility of multiple side chain/main chain hydrogen bonds and χ_1 conformational heterogeneity.[17] The lowest PPII propensities are observed for aromatic amino acids and for sterically hindered β-branched amino acids (Thr, Ile, Val, and particularly the highly sterically congested *tert*-leucine (Tle)), indicating that steric hindrance near the protein backbone strongly opposes PPII.

All peptides were analyzed by circular dichroism. In $tau_{174–183}$ (Figure 3), which contains the Alzheimer's disease phosphoepitope pThr175/pThr181, the phosphorylated peptide was observed to have greater PPII (larger signal at 228 nm, a defined maximum indicative of PPII) than the nonphosphorylated peptide.[7,15a,18] Interestingly, the CD of the phosphorylated peptide was similar to the peptide with both threonines changed to the phosphomimic (and PPII-favoring residue) Glu, although the structural effect of replacement of Thr by Glu was less than that of Thr phosphorylation (Figure 3b). In contrast, the OGlcNAcylated peptide exhibited reduced PPII compared to the nonphosphorylated peptide, indicating that OGlcNAcylation disfavors PPII.[19] The effect of diethylphosphorylation was qualitatively similar to that of OGlcNAcylation, though greater in magnitude. The structural change of OGlcNAcylation was also observable in a red shift of the λ_{max} of the CD

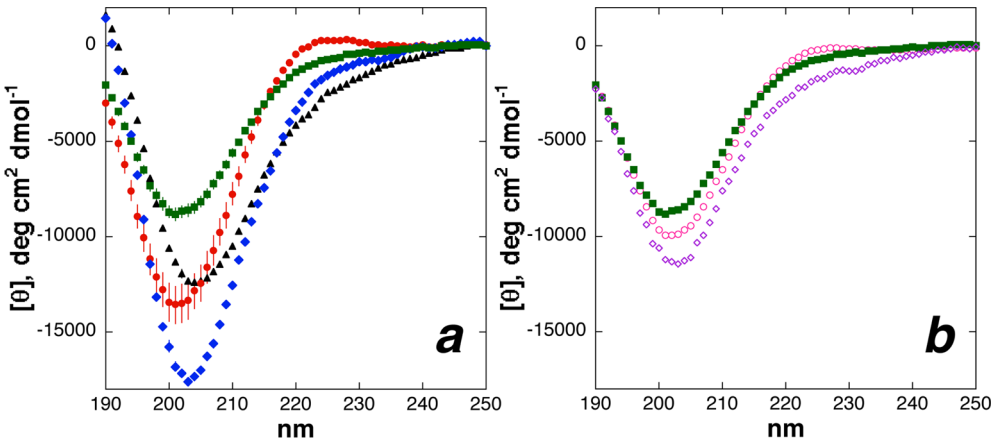

Figure 3. CD spectra of $tau_{174–183}$ peptides (Ac–K**T**PPAPK**T**PP-NH_2) in water with 5 mM phosphate buffer and 25 mM KF at pH 7.5. (a) Thr, green squares; phosphothreonine, red circles; ThrOGlcNAc, blue diamonds; ThrOPO_3Et_2, black triangles. (b) Peptides with Thr (green squares) or with both Thr residues replaced by either Glu (Ac–K**E**PPAPK**E**PP-NH_2) (magenta open circles) or *tert*-leucine (Tle) (Ac–K**Tle**PPAPK**Tle**PP-NH_2) (purple open diamonds).

dx.doi.org/10.1021/ja407156m | J. Am. Chem. Soc. 2014, 136, 3803–3816

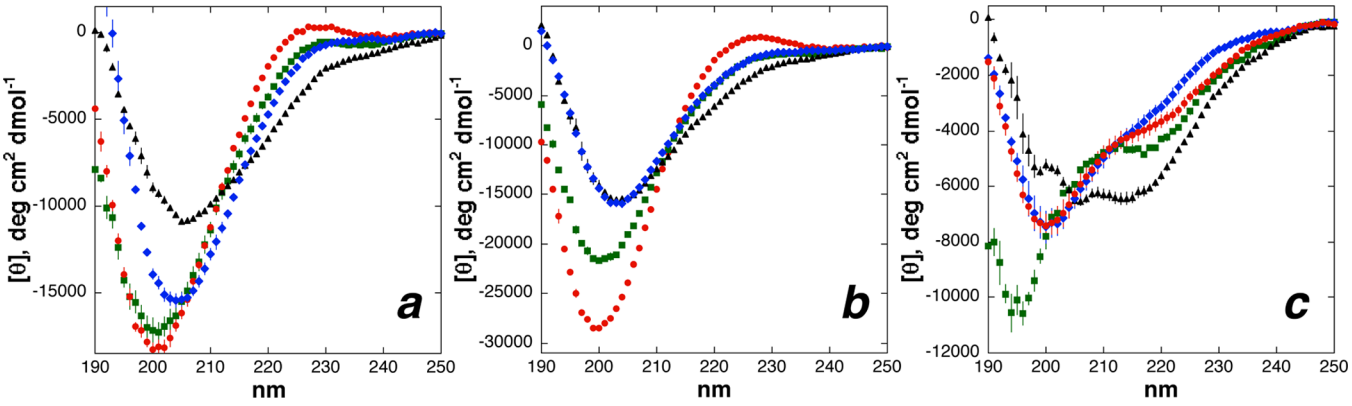

Figure 4. CD spectra of (a) $tau_{211–219}$, (b) $tau_{229–238}$, and (c) $tau_{196–209}$ peptides in water with 5 mM phosphate buffer and 25 mM KF at pH 7.5. Unmodified Ser/Thr, green squares; phosphoserine/phosphothreonine, red circles; Ser/Thr OGlcNAc, blue diamonds; Ser/Thr OPO_3Et_2, black triangles.

minimum, from 201 nm in the phosphorylated peptide to 203 nm in the OGlcNAcylated peptide and to 204 nm in the diethylphosphorylated peptide, as well as in a greater mean residue ellipticity at 190 nm for the OGlcNAcylated peptide. Data on the OGlcNAc and diethylphosphate peptides were similar to those of a polyproline helix negative control, with the threonines replaced by the sterically demanding *tert*-leucine.[7,15a]

Similar opposing effects of phosphorylation versus OGlcNAcylation were also observed in other proline-rich peptides exhibiting residual PPII structure ($tau_{211–219}$, $tau_{229–238}$), with phosphorylation inducing PPII and OGlcNAcylation opposing PPII (Figure 4a,b). These peptides include the sites of several major tau phosphoepitopes (pThr212, pSer214, and pThr231) that are observed pathologically in Alzheimer's disease. The reduction in PPII for the OGlcNAcylated and diethylphosphorylated peptides, particularly compared to the phosphorylated peptides, was observable in reduced mean residue ellipticity at 228 nm, in a red shift in the minimum around 200 nm, and in increased mean residue ellipticity at 190 nm.

In contrast, the structural effects of OGlcNAcylation and phosphorylation were not distinct in $tau_{196–209}$, although, interestingly, peptides with both post-translational modifications were different from the unmodified peptide (Figure 4c). In $tau_{196–209}$, both OGlcNAcylation and phosphorylation disrupted a nascent α-helix CD signature (minimum in CD ~220 nm) in the unmodified peptides. This sequence is less proline-rich than the other peptides examined (3 Pro in 14 residues), and includes three consecutive PG(S/T) repeats. PGSPG(S/T) sequences in the PDB are observed as α-helix nucleation sites, with the Ser side chain and SPG(S/T) main chain oxygens acting as hydrogen bond acceptors to nucleate (N-cap) the N-terminus of an α-helix (e.g., glutaminyl cyclase (pdb 3si0), interleukin-5 receptor (pdb 3qt2)).[20] Phosphorylation has been observed to disrupt α-helix formation when the phosphorylation site is at an internal site in α-helices.[21] In contrast to the results above, in this case, the diethylphosphate, which induced increased α-helix, was structurally divergent from OGlcNAcylation. The observation here of similar effects of phosphorylation and OGlcNAcylation on α-helicity emphasizes the importance of structural context in understanding the effects of phosphorylation and OGlcNAcylation. Indeed, while in many cases phosphorylation and OGlcNAcylation are functionally opposing, in some cases OGlcNAcylation and phosphorylation result in similar functional effects in proteins.[2]

In order to identify whether the structural effects of post-translational modifications seen in smaller peptides were also observed in a broader structural context, we examined the peptide $tau_{211–238}$. This peptide contains six phosphorylation sites, incorporating two proline-rich regions (residues 211−219 and 229−238) separated by a hydrophobic segment (the "B" domain of Figure 2, including the highly hydrophobic VAVV motif). By circular dichroism, phosphorylation of $tau_{211–238}$ induced an increase in mean residue ellipticity at 228 nm, consistent with induced polyproline helix upon tau phosphorylation in data seen in smaller peptides above (Figure 5). The

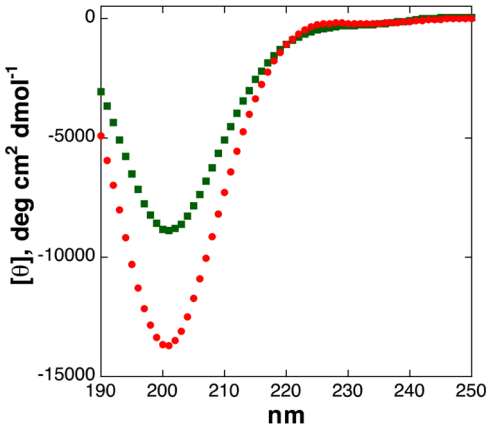

Figure 5. CD spectra of unmodified (green squares) and phosphorylated (red circles) $tau_{211–238}$ at 0.5 °C in water with 5 mM phosphate buffer pH 8 and 25 mM KF.

magnitude of the increase in mean residue ellipticity at 228 nm was substantially less than seen in smaller peptides, and cannot be definitively structurally assigned in the larger peptide, but is consistent with an equivalent change in structure to polyproline helix within the proline-rich segments. The magnitude of the change in mean residue ellipticity is smaller because of the larger number of residues in the peptide, including residues not affected by the local structural organization induced by phosphorylation (signal dilution by other residues in the peptide, including B domain residues that adopt an extended conformation in tau[18]). The data from these peptides confirm induced polyproline helix upon phosphorylation in larger

dx.doi.org/10.1021/ja407156m | J. Am. Chem. Soc. 2014, 136, 3803−3816

peptides but emphasize the difficulty in identifying polyproline helix in larger peptides and the special utility of smaller peptides for definitively identifying polyproline helix.

One additional peptide, $tau_{234-251}$ (Figure 2), was examined by circular dichroism. Landrieu and Lippens identified via $^{13}C\alpha$ chemical shift index[22] analysis that enzymatic phosphorylation of a tau protein fragment (residues 208−324) by cdk2/cyclinA3, including phosphorylation at Ser235, resulted in an increase in $^{13}C\alpha$ chemical shift consistent with a small induction of α-helix in residues 236−239 of tau.[5e] Analysis of the tau sequence suggests a short segment between residues 235 and 246 with the potential to form an α-helix, with the sequence bounded by prolines at residues 236 and 247 serving as α-helix start and stop signals.[23] The C-terminal prolines at residues 247, 249, and 251 are expected to strongly prevent α-helix propagation beyond residue 246, although the $P_{247}VPMP_{251}$ sequence could potentially function as a hydrophobic α-helix C-cap. CD experiments revealed a very weak α-helical signature in the nonphosphorylated peptide, with modestly increased α-helicity in trifluoroethanol (TFE) (Figure 6, Figure S6, Supporting Information).[24] These data are consistent with analysis of Griesinger, Mandelkow, Zweckstetter, and co-workers, who found that residues 240−251 of nonphosphorylated tau do not adopt a well-defined conformation,[5e,18,25] and that residues 232−239 predominantly adopt a polyproline helix conformation, as we observed above and previously[7] for $tau_{229-238}$ and $tau_{229-242}$. Phosphorylation of Ser235 resulted in a small increase in α-helicity of this peptide, consistent with the results of Landrieu and Lippens, with a greater α-helical induction observed in the α-helix-promoting solvent TFE.[24] In contrast, phosphorylation at both Ser235 and Ser237, in addition to exhibiting a weak α-helical signature, induced a small positive band at ∼225 nm consistent with the local induction of polyproline helix around these residues that was seen in $tau_{229-238}$. Overall, these results are consistent with the expected low α-helicity of this peptide sequence, whose α-helicity is hampered by a short sequence of potential α-helical character (12 residues; Pro has good α-helical propensity only at the first and second residues of an α-helix[26]), multiple residues with low α-helix propensity (3 Ser and a Thr within the central 10 residues between the prolines), and a C-terminal proline residue, which prevents continuation of the hydrogen-bonding pattern of the α-helix and substantially reduces α-helical content of short α-helical peptides.[23b,d,27] Notably, the α-helical content and induced α-helicity could be substantially greater in the dynamic presence of transient tertiary structure present in tau.[4,18,28]

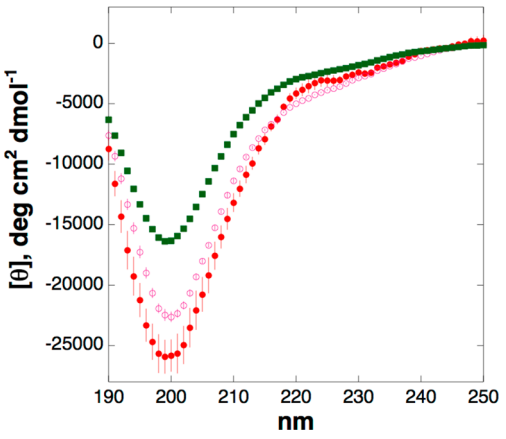

Figure 6. CD spectra of unmodified (green squares), monophosphorylated at Ser235 (magenta open circles), and doubly phosphorylated (at Ser235/Ser237) (red circles) $tau_{234-251}$ at 25 °C in water with 5 mM phosphate buffer pH 8 and 25 mM KF.

To understand the structural basis for the observed opposing conformational effects of OGlcNAcylation versus phosphorylation in proline-rich motifs, all tau peptides were examined by NMR spectroscopy. In addition to analysis of tau peptides, the effects of post-translational modifications were examined within the simple $tau_{174-183}$-derived model peptide Ac-KXPP-NH_2 (X = Ser, Thr, or phosphorylated or OGlcNAcylated Ser or Thr), whose sequence (with Thr) is repeated twice in $tau_{174-183}$ ($K_{174}TPP_{177}$ and $K_{180}TPP_{183}$) and which is homologous to the $R_{230}TPP_{233}$ sequence in $tau_{229-238}$. This peptide was also applied to examine the effects of threonine versus serine modification. In addition, the structural effects of phosphorylation versus OGlcNAcylation were also examined within the model peptide Ac-GPPXPPGY-NH_2 context, which was previously used to identify polyproline helix propensity,[15a] and in the related proline-rich peptide Ac-GPKXPPGY-NH_2, which contains the KTPP sequence present in $tau_{174-183}$ (for

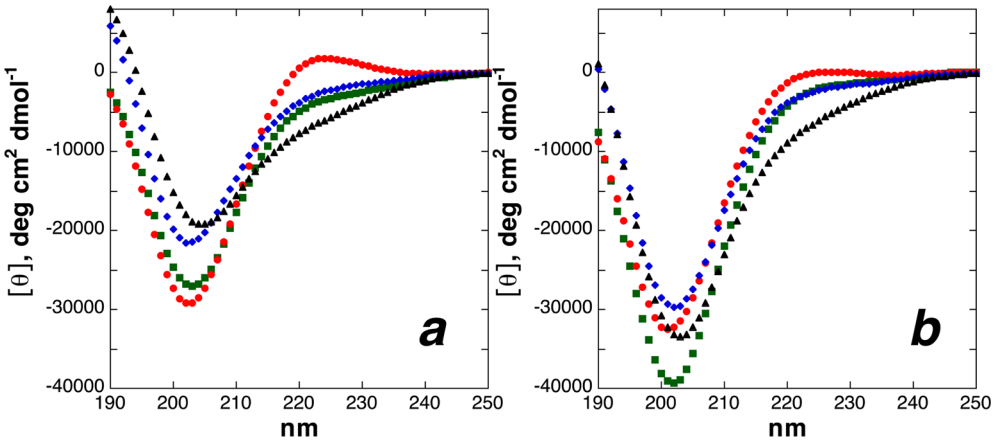

Figure 7. CD spectra of (a) Ac-KTPP-NH_2 and (b) Ac-KSPP-NH_2 peptides at 25 °C in water with 5 mM phosphate pH 8 and 25 mM KF. Unmodified Ser/Thr, green squares; phosphoserine/phosphothreonine, red circles; Ser/Thr OGlcNAc, blue diamonds; Ser/Thr OPO_3Et_2, black triangles. Data on these peptides at 2 °C, where greater PPII is observed, are in the Supporting Information (Figure S11).

dx.doi.org/10.1021/ja407156m | J. Am. Chem. Soc. 2014, 136, 3803−3816

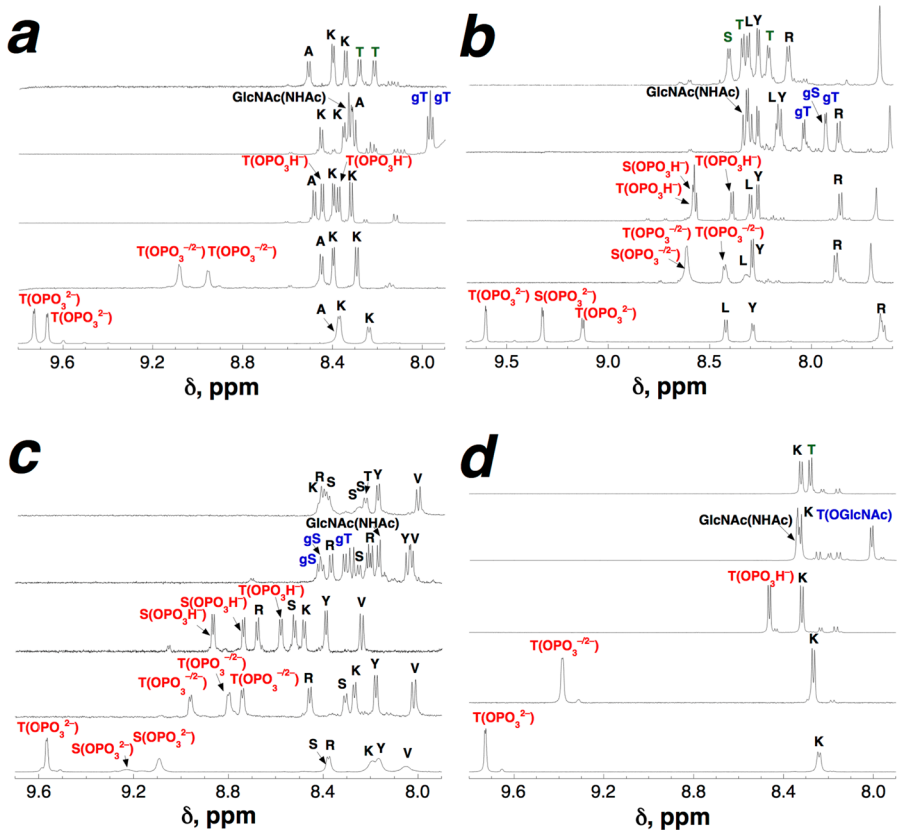

Figure 8. 1-D NMR spectra (amide region) of peptides with Ser/Thr, Ser/Thr(OGlcNAc), Ser/Thr(OPO_3H^-) (pH 4), Ser/Thr($OPO_3(H)^{-/2-}$) (pH 6.5), and Ser/Thr(OPO_3^{2-}) (pH 8). Experiments were conducted at 298 K in 90% H_2O/10% D_2O with 5 mM phosphate (pH 4 or as indicated) and 25 mM NaCl. gS and gT indicate the resonances of the SerOGlcNAc and ThrOGlcNAc, respectively, backbone amide protons. GlcNAc(NHAc) indicates the sugar amide proton. (a) $tau_{174-183}$ peptides; (b) $tau_{211-219}$ peptides; (c) $tau_{229-238}$ peptides; (d) Ac-KTPP-NH_2 peptides.

Table 1. Ser/Thr NMR Data at 298 K for Peptides[a]

		$^3J_{\alpha N}$, Hz				
peptide	residue	ROH	$ROPO_3H^-$	$ROPO_3^{2-}$	ROGlcNAc	$ROPO_3Et_2$
$tau_{174-183}$	Thr	7.3, 7.3	6.7, 6.3	3.8, 3.5	7.5, 7.5	n.d.
$tau_{211-219}$	Thr	7.0, 6.4	6.7, 6.6	3.7, 3.1	5.7, 4.2	7.0, 6.8
	Ser	6.5	n.d.	5.5	7.8	7.3
$tau_{229-238}$	Thr	7.3	7.1	3.7	6.5	5.9
	Ser	n.d.	6.4, 6.4	5.3, 5.2	8.0, 6.9	7.4, 7.0
GPPTPPGY	Thr	7.3	6.5	3.5	5.9	7.9
GPKTPPGY	Thr	7.4	6.7	3.5	6.7	8.3
KTPP	Thr	7.2	6.1	3.5	6.4	8.4
KSPP	Ser	6.8	6.5	5.5	6.4	7.6
mean	Ser	6.8	6.4	5.4	7.3	7.3
	Thr	7.2	6.6	3.5	6.3	7.4

[a] $^3J_{\alpha N}$ values < 6 Hz correlate with compact and ordered conformations, values > 8 Hz indicate extended conformations, and values between 6 and 8 Hz are observed in disordered peptides. In general, smaller $^3J_{\alpha N}$ values indicate more compact conformations, while larger $^3J_{\alpha N}$ values indicate more extended conformations. $tau_{196-209}$ is not included here because of spectral overlap. n.d. = not determined due to spectral overlap. Glu $^3J_{\alpha N}$ values in $tau_{174-183}$(Thr → Glu) are 6.6 and 5.8 Hz. *tert*-Leucine $^3J_{\alpha N}$ values in $tau_{174-183}$(Thr → Tle) are 8.8 and 7.9 Hz. In Ac-GPPXPPGY-NH_2 peptides, the $^3J_{\alpha N}$ value of Glu is 6.3 Hz, the third most-restricted value for canonical amino acids after Ala (5.7 Hz) and Asp (6.2 Hz), while that of *tert*-leucine is 8.3 Hz, larger than all canonical amino acids (Val 8.0 Hz, Ile 7.9 Hz) and indicative of a strong preference for the extended conformation.[15a] Data on phosphorylated peptides were obtained at pH 4 ($ROPO_3H^-$) or pH 8 ($ROPO_3^{2-}$) (typical phosphoserine/phosphothreonine pK_a 5.5−6.0). Additional NMR data for all peptides are in the Supporting Information.

these peptides, X = ThrOH, $ThrOPO_3^{2-}$, $ThrOPO_3Et_2$, and ThrOGlcNAc).

In these proline-rich model peptides, similar conformational effects of post-translational modifications were observed by CD as were found in proline-rich tau peptides, with phosphorylation increasing PPII and OGlcNAcylation and diethylphosphorylation opposing PPII (Figure 7, Figures S7−S17, Tables S5−S7, Supporting Information). Notably, comparison of the CD spectra of KTPP and KSPP peptides (Figure 7, Figures S7−S11, Tables S5 and S6, Supporting Information) revealed a

dx.doi.org/10.1021/ja407156m | J. Am. Chem. Soc. 2014, 136, 3803−3816

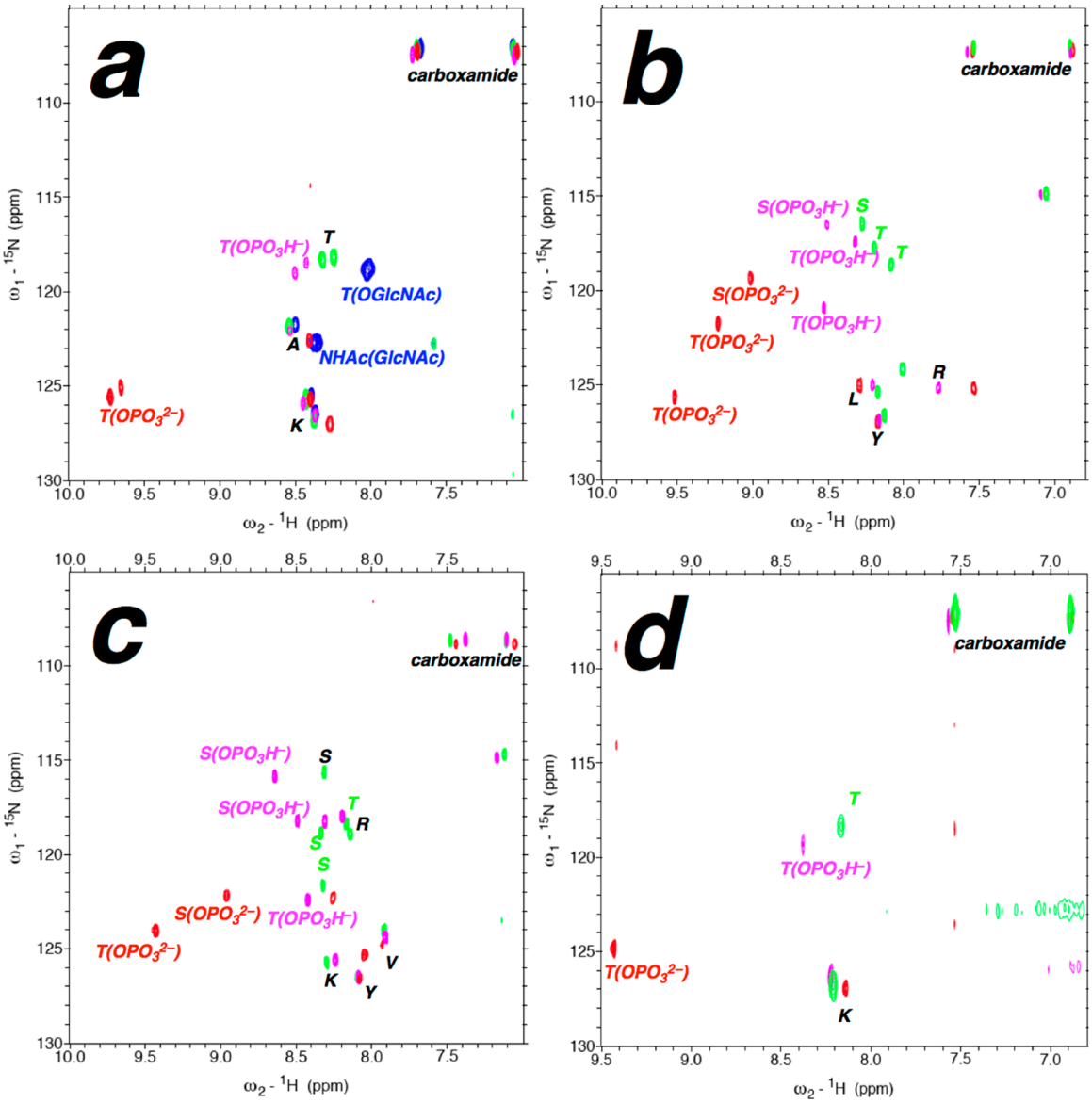

Figure 9. $^{1}H-^{15}N$ HSQC spectra of (a) $tau_{174-183}$, (b) $tau_{211-219}$, (c) $tau_{229-238}$, and (d) Ac-KTPP-NH_2 peptides. Green, peptides with unmodified Ser/Thr; blue, peptides with Thr(OGlcNAc); magenta, peptides with Ser/Thr(OPO_3H^-) (pH 4); red, peptides with Ser/Thr(OPO_3^{2-}) (pH 8).

substantially larger structural change for Thr phosphorylation than Ser phosphorylation ($\Delta[\theta]_{224}$ = +5310 and +2230 deg cm^2 $dmol^{-1}$ for pThr−Thr and pSer−Ser, respectively). The larger change in structure upon Thr phosphorylation than Ser phosphorylation was both due to lower population of PPII for the peptide with Thr than with Ser and due to greater PPII with pThr than with pSer. These data suggest that substantially larger structural changes are induced because of threonine phosphorylation than because of serine phosphorylation.

Data on polyproline helix model peptides Ac-GPPTPPGY-NH_2 and Ac-GPKTPPGY-NH_2 peptides were similarly consistent with data in tau peptides. Data from Ac-GPPpTPPGY-NH_2 also indicated no effect of 2 mM $MgCl_2$ on the CD spectra (and thus, no substantial effect of Mg^{2+} on structure) of phosphorylated peptides. In addition, a greater mean residue ellipticity at 228 nm was observed at 2 °C than at 25 °C, consistent with the interpretation that these CD data are specifically indicative of PPII content in the peptides, as was previously seen in other proline-rich and polyproline helix-containing peptides.[7,15a−c,16a,e]

A series of homonuclear (1-D ^{1}H and TOCSY) and heteronuclear ($^{1}H-^{15}N$ HSQC, $^{1}H-^{13}C$ HSQC, and $^{1}H-^{13}C$ HMBC) NMR experiments was conducted on tau-derived peptides and proline-rich model peptides to identify residue-specific and post-translational-modification-specific changes in structure (Figures 8−11, Tables 1−4). NMR data in this series of peptides were consistent with CD data, indicating that phosphorylation in proline-rich sequences induces structural changes leading to more compact and more ordered conformations, whereas OGlcNAcylation and diethylphosphorylation exhibited evidence of more extended conformations, as expected for sterically demanding amino acids in proline-rich domains.[7,15a−c,16e] 1-D ^{1}H NMR spectroscopy indicated substantial divergence of the peptides that was a function of post-translational modification: across all peptides, relative to unmodified Ser/Thr, phosphorylation induced downfield amide chemical shifts and smaller $^{3}J_{\alpha N}$ for phosphorylated residues; in

dx.doi.org/10.1021/ja407156m | J. Am. Chem. Soc. 2014, 136, 3803−3816

Table 2. Mean ^{1}H Chemical Shifts (ppm) for Serine/Threonine Resonances Across All Peptides as a Function of Side Chain and Post-Translational Modification[a]

	H^N				Hα				Hβ			
	OH	OGlcNAc	OPO_3H^-	OPO_3^{2-}	OH	OGlcNAc	OPO_3H^-	OPO_3^{2-}	OH	OGlcNAc	OPO_3H^-	OPO_3^{2-}
Ser	8.32	8.31	8.62	8.99	4.50	4.50	4.68	4.63	3.87	3.79	4.13	4.05
Thr	8.23	8.01	8.43	9.63	4.56	4.55	4.63	4.35	4.11	4.12	4.43	4.27

[a]Full tabulated NMR data and statistical analysis are in the Supporting Information.

contrast, OGlcNAcylation of Thr residues induced upfield amide chemical shifts and amide chemical shifts similar to those of Ser for SerOGlcNAc. In addition, experiments on non-phosphorylated and phosphorylated $tau_{211-238}$ indicated that the large amide chemical shift changes and conformational restriction observed for phosphoresidues in $tau_{211-219}$ and $tau_{229-238}$ peptides were also observed in the larger peptide context (Figures S54 and S55, Supporting Information). Of particular note, in all peptides, phosphorylated residues exhibited substantially downfield (δ = 9.4−9.8 ppm as $ThrOPO_3^{2-}$, 8.7−9.2 ppm as $SerOPO_3^{2-}$) amide proton chemical shifts, with amide proton chemical shifts substantially more downfield for the dianionic than the monoanionic phosphates (monoanionic pSer/pThr δ = 8.35−8.75 ppm) (Figures 8 and 9, Table 2, Table S36, Supporting Information), as has been observed previously in some peptides and proteins.[5a,c,e,29]

Phosphorylated Ser/Thr residues in these peptides were particularly conformationally restricted. $^3J_{\alpha N}$ values correlate with the ϕ backbone torsion angle via a parametrized Karplus equation, with values between 6 and 8 Hz consistent with disorder or averaging of multiple conformations, values > 8 Hz indicative of ordered, extended conformations, and values < 6 Hz indicative of ordered, compact conformations, and more broadly with smaller values indicating more compact conformations, larger values indicating more extended conformations, and values further from random coil values indicating greater extent of order.[30] The $^3J_{\alpha N}$ values observed are indicative of special conformational order for the phosphorylated residues: across all peptides, dianionic phosphothreonine exhibits a mean $^3J_{\alpha N}$ = 3.5 Hz, corresponding to $\phi = -55°$, compared to a random coil value for Thr ($^3J_{\alpha N}$ = 7.2 Hz, average $\phi = -83°$); dianionic phosphoserine exhibits a mean $^3J_{\alpha N}$ = 5.4 Hz, corresponding to average $\phi = -70°$, compared to a random coil value for Ser ($^3J_{\alpha N}$ = 6.8 Hz, average $\phi = -80°$)) (Table 1).[30] Notably, the substantial conformational order induced by phosphorylation was dependent on the dianionic phosphates: only small increases in order were induced by monoanionic phosphoserine ($^3J_{\alpha N}$ = 6.4 Hz), phosphothreonine ($^3J_{\alpha N}$ = 6.6 Hz), and glutamic acid ($^3J_{\alpha N}$ = 6.2 Hz). Interestingly, the small coupling constants for dianionic phosphorylated amino acids observed herein are also consistent with a growing number of examples of proteins in which phosphorylation induces α-helix formation when at its N-terminus.[5e,21b,29a,31]

^{1}H−^{15}N HSQC experiments indicated that, in addition to large downfield changes in the chemical shifts of amide protons, the serine/threonine amide nitrogens exhibited large downfield changes in chemical shift upon phosphorylation across all peptides (Figure 9, Table 3; tabulated data Table S39, Supporting Information). In $tau_{174-183}$, the dianionic phosphothreonine amide nitrogens were 7.2 ppm downfield of the amides of threonine and 6.6 ppm downfield of the amides of monoanionic phosphothreonine. In contrast, OGlcNAcylated

Table 3. Mean Amide ^{15}N Chemical Shifts (ppm) for Serine/Threonine Resonances Across All Peptides as a Function of Side Chain and Post-Translational Modification[a]

	OH	OPO_3H^-	OPO_3^{2-}	$\Delta\delta^b$
Ser	118.2	116.9	120.8	2.6
Thr	118.1	119.3	124.3	6.2

[a]Full tabulated NMR data and statistical analysis are in the Supporting Information. [b]$\Delta\delta = \delta$ (Ser/Thr(OPO_3^{2-})) − δ (Ser/Thr(OH)).

threonine exhibited amide nitrogen chemical shifts only 0.6 ppm downfield of those of threonine. The large divergence in amide nitrogen chemical shift between monoanionic and dianionic phosphothreonine is not consistent with differences in the electron-withdrawing nature of the different protonation states of these phosphates,[13b,32] suggesting that these differences are due to particular structure induced by dianionic phosphothreonine, consistent with differences in $^3J_{\alpha N}$ values between monoanionic and dianionic phosphopeptides. ^{1}H−^{15}N HSQC data from other proline-rich peptides ($tau_{211-219}$, $tau_{229-238}$, and Ac-KTPP-NH_2) exhibited similar trends, with large downfield changes in amide hydrogen and amide nitrogen resonances for dianionic phosphoresidues compared to the monoanionic phosphoresidues or unmodified Ser/Thr [amide nitrogens: $tau_{211-219}$ $\Delta\delta_{mean}$ = +0.1 and +1.0 ppm for monoanionic phosphoserine and phosphothreonine, respectively, compared to unmodified Ser/Thr, versus $\Delta\delta_{mean}$ = +2.9 and +5.5 ppm for dianionic phosphoserine and phosphothreonine, respectively, compared to unmodified Ser/Thr; $tau_{229-238}$ $\Delta\delta_{mean}$ = +2.6 ppm (pSer(OPO_3^{2-})) and +5.6 ppm (Thr(OPO_3^{2-})) ppm for the dianionic phosphoresidues compared to the unmodified Ser/Thr; Ac-KTPP-NH_2 $\Delta\delta$ = +1.1 ppm (pThr(OPO_3H^-)) and $\Delta\delta$ = +6.5 ppm (pThr(OPO_3^{2-})) relative to unmodified Thr; Ac-GPPTPPGY-NH_2, $\Delta\delta$ = +0.1 ppm (pThr(OPO_3H^-)) and $\Delta\delta$ = +6.2 ppm (pThr(OPO_3^{2-})) relative to unmodified Thr]. Collectively, these data demonstrate very large induced changes in the electronic environment around the amide nitrogens of dianionic phosphoserine and dianionic phosphothreonine residues compared to Ser/Thr, Ser/Thr(OGlcNAc), or to monoanionic phosphoserine or phosphothreonine.

Notably, small downfield changes in amide nitrogen chemical shift are associated with the polyproline helix conformation ($\Delta\delta$ = +1.1 ppm for change from random coil to polyproline helix).[16e] While the changes in phosphoserine/phosphothreonine amide chemical shifts are too large to be explained by secondary structure, most other resonances in these peptides also exhibited small downfield changes in ^{15}N amide chemical shift upon phosphorylation, consistent with the increased PPII seen by CD (Figure 10; tabulated data in the Supporting Information). In contrast, the amides of OGlcNAcylated $tau_{174-183}$ exhibited small upfield changes in ^{15}N chemical shift, consistent with the reduced PPII seen in this peptide.

dx.doi.org/10.1021/ja407156m | J. Am. Chem. Soc. 2014, 136, 3803−3816

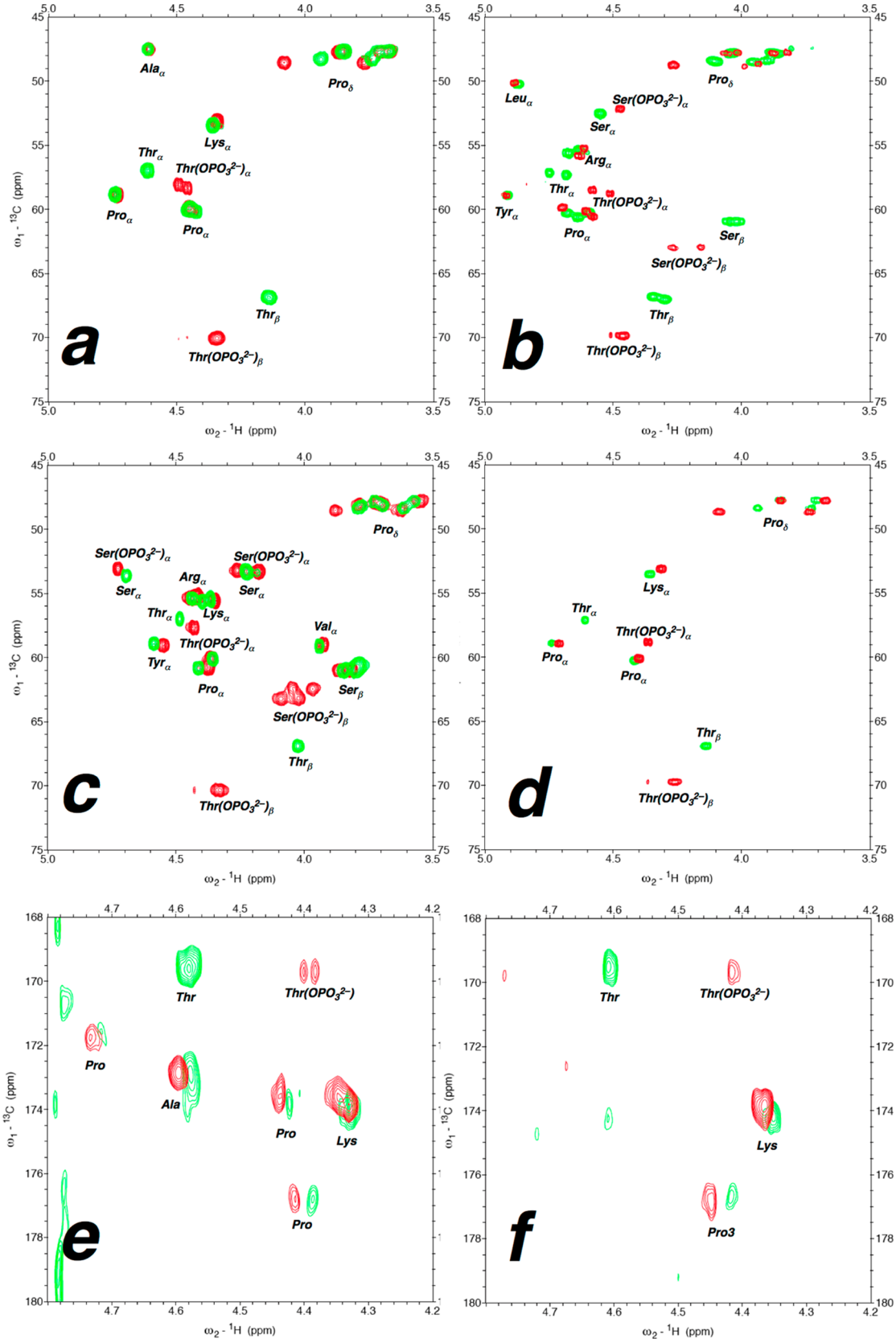

Figure 10. (a–d) ^{1}H–^{13}C HSQC spectra (Hα–Cα region) of (a) tau$_{174–183}$, (b) tau$_{211–219}$, (c) tau$_{229–238}$, and (d) Ac-KTPP-NH$_2$ peptides. (e,f) ^{1}H–^{13}C HMBC spectra (Hα—C═O region) of (e) tau$_{174–183}$ and (f) Ac-KTPP-NH$_2$ peptides. Green, peptides with unmodified Ser/Thr; red, peptides with Ser/Thr(OPO$_3^{2-}$) (pH 8). Full spectra and tabulated data are in the Supporting Information.

^{1}H–^{13}C HSQC experiments were conducted on tau peptides to further characterize the residue-specific effects of protein phosphorylation (Figure 10, Table 4). In addition, to determine the effects of phosphorylation on the backbone carbonyls,

dx.doi.org/10.1021/ja407156m | J. Am. Chem. Soc. 2014, 136, 3803–3816

Table 4. Mean ^{13}C Chemical Shifts (ppm) for Serine/Threonine Resonances Across All Peptides as a Function of Side Chain and Post-Translational Modification[a]

	$^{13}C\alpha$			$^{13}C\beta$		
	OH	OPO_3^{2-}	$\Delta\delta$[b]	OH	OPO_3^{2-}	$\Delta\delta$
Ser	53.3	53.0	−0.3	60.7	62.6	1.9
Thr	57.1	58.4	1.3	66.9	70.0	3.1

[a]Full tabulated NMR data and statistical analysis are in the Supporting Information. [b]$\Delta\delta = \delta$ (Ser/Thr(OPO_3^{2-})) − δ (Ser/Thr(OH)).

$^1H-^{13}C$ HMBC experiments were conducted on nonphosphorylated and phosphorylated $tau_{174-183}$ and the model peptide Ac-KTPP-NH_2 (Figure 10e,f). PPII, in contrast to α-helix or β-sheet, does not exhibit large changes in Hα ($\Delta\delta$ = −0.03 ppm), Cα ($\Delta\delta$ = +0.3 ppm), or C=O ($\Delta\delta$ = +0.1 ppm) chemical shift compared to random coil.[16e] These experiments revealed large changes in the ^1H and ^{13}C chemical shifts of phosphorylated residues, as expected because of the electronic change of the side chain, though with substantially larger chemical shift changes at phosphothreonine than at phosphoserine (Table 3). In particular, as the dianion, phosphorylation of serine induced downfield shifts in Hα ($\Delta\delta$ = +0.13 ppm) and upfield shifts in Cα ($\Delta\delta$ = −0.3 ppm), in contrast to upfield shifts in Hα ($\Delta\delta$ = −0.21 ppm) and downfield shifts in Cα ($\Delta\delta$ = +1.3 ppm) for phosphorylation of threonine. Data from other residues, within the context of the small inherent changes in chemical shift for PPII, also indicated that the structural changes upon phosphorylation propagated to residues beyond the phosphorylated residues (Figure 10).[33] One defining feature stabilizing the polyproline helix is an n → π^* interaction between adjacent carbonyls.[34] The observation of changes in the carbonyl chemical shifts across all residues (including the N-terminal acetyls) is consistent with phosphorylation-induced changes in the environment around the backbone carbonyls of all residues in the peptides.

Peptides with phosphorylated amino acids also exhibited relatively slow amide hydrogen exchange considering the absence of tertiary structure or hydrogen-bonded secondary structure, with most amide protons observable at pH 8 for phosphorylated proline-rich peptides (Figure 8, Supporting Information). For the peptide Ac-KT(OPO_3^{2-})PP-NH_2, slow amide exchange, small $^3J_{\alpha N}$ values, and downfield pThr amide chemical shifts at pH 8 were persistent even at elevated temperature (up to 323 K) and at high salt concentrations (up to 1 M NaCl) (Figure 11). These data are consistent with a strong interaction that is in slow exchange and that cannot be readily screened electrostatically, suggesting that the induced structure is not primarily due to a simple lysine-phosphate or arginine-phosphate electrostatic interaction of the phosphorylated residue with the prior basic residue. These data on dianionic phosphorylated amino acids are particularly striking, since in disordered peptides, amide protons are generally not observed or are substantially exchange-broadened at pH 8. Slow amide exchange on the NMR time scale at pH 8 is generally associated with more stable structures (e.g., those involving hydrogen bonding, an interaction that could slow amide exchange at the pSer/pThr amides, though not other amides).[29d,e,35] While PPII does not exhibit hydrogen bonding, PPII is stabilized by n → π^* interactions between adjacent carbonyls, which could also potentially slow exchange of the amide protons.[34a−d,36]

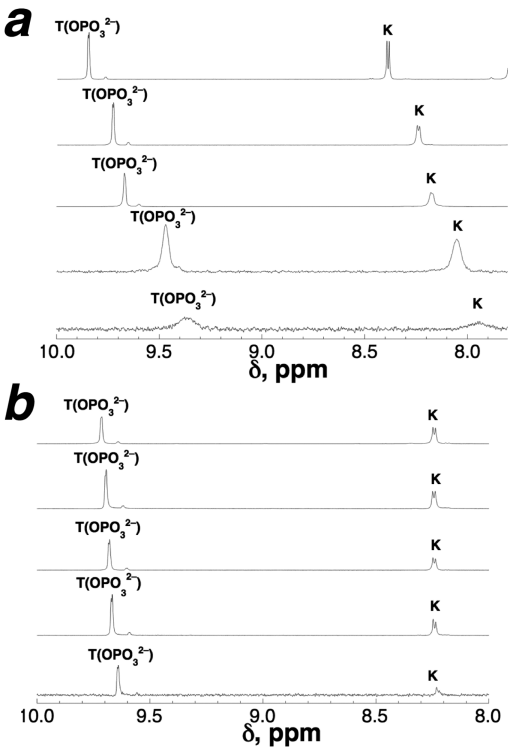

Figure 11. (a) Temperature-dependent ^1H NMR spectra of Ac-KT(OPO_3^{2-})PP-NH_2. Experiments were conducted in 90% H_2O/10% D_2O with 5 mM phosphate buffer and 25 mM NaCl at pH 8.0. Experiments were conducted at 277 (top), 298, 308, 323, and 338 K (bottom). Experiments at 277, 298, and 308 K were conducted on a 600 MHz cryoprobe instrument, while experiments at 323 and 338 K were conducted on a 400 MHz instrument. (b) Salt-dependent ^1H NMR spectra of Ac-KT(OPO_3^{2-})PP-NH_2. Experiments were conducted in 90% H_2O/10% D_2O in 5 mM phosphate buffer at pH 8.0 with 25 (top), 125, 225, 325, and 1000 (bottom) mM NaCl.

Interestingly, by NMR, the effects of modifications on serine versus threonine were divergent in magnitude (Tables 1−4), as had been seen by CD above in Ac-KXPP-NH_2 peptides (Figure 5). Greater overall conformational restriction ($^3J_{\alpha N}$) was observed at phosphothreonine than at phosphoserine, as well as a larger change in $^3J_{\alpha N}$ (and thus in the main chain torsion angle ϕ) between the nonphosphorylated and phosphorylated peptides (mean $\Delta^3J_{\alpha N}$ = 3.7 Hz for Thr, versus 1.4 Hz for Ser). Phosphothreonine amide protons also exhibited greater downfield shifts than phosphoserine amides (mean amide δ 9.63 ppm for dianionic pThr, versus 8.99 ppm for dianionic pSer, compared to 8.23 and 8.32 ppm for Thr and Ser; $\Delta\delta_{mean}$ = +1.40 ppm for threonine phosphorylation, versus $\Delta\delta_{mean}$ = +0.67 ppm for serine phosphorylation (Table 2)), as well as greater downfield shifts in amide nitrogens (mean amide δ 124.3 ppm for dianionic pThr, versus 120.8 ppm for dianionic pSer, compared to 118.1 and 118.2 ppm for Thr ($\Delta\delta_{mean}$ = +6.2 ppm) and Ser ($\Delta\delta_{mean}$ = +2.6 ppm), respectively) (Table 3). Larger changes in chemical shifts were also observed for threonine phosphorylation than serine phosphorylation on Hα, Cα, and Cβ (Table 2, Table 4, Tables S37 and S40, Supporting Information). Collectively, these data are consistent with a stronger phosphate-amide interaction in phosphothreonine than phosphoserine and greater induced structural changes for phosphothreonine than phosphoserine. Notably, threonine and serine residues are differentially phosphorylated and dephosphorylated in vivo, and evolution of Thr and Ser

dx.doi.org/10.1021/ja407156m | J. Am. Chem. Soc. 2014, 136, 3803−3816

residues occurs at different rates, suggesting native functional differences between Thr and Ser.[37]

DISCUSSION

We have described the direct comparison of the structural effects of phosphorylation versus OGlcNAcylation, competing intracellular protein post-translational modifications that often occur on the same Ser/Thr residues, on peptide conformation within a typical natively disordered protein context.[2,18,38] This work was specifically applied within the context of the tau protein, where hyperphosphorylation is associated with protein misfolding and aggregation, but OGlcNAcylation is protective against protein misfolding.[3a,5d,8−10] We found that within proline-rich sequences phosphorylation promotes conformational order and PPII formation, whereas OGlcNAcylation or modification with the practical OGlcNAc mimic of diethylphosphorylation leads to conformational preference against PPII and a more disordered or extended conformation. The effects of phosphorylation and OGlcNAcylation are divergent: whereas phosphorylation induces significant conformational order, particularly on threonine residues, the effects of OGlcNAcylation are more subtle, confirming the strong conformational biases of serine and threonine against PPII. Interestingly, in the RNA polymerase II C-terminal domain repeat (SYSPTSPS), phosphorylation promotes binding to the Pin1 WW domain as a polyproline helix, whereas Thr OGlcNAcylation induces a more extended conformation, consistent with results on tau peptides herein.[19] As phosphorylation and OGlcNAcylation are competing protein intracellular post-translational modifications, which generally occur on disordered protein sequences, these data suggest potentially general opposing modes of structural changes due to these post-translational modifications.[39]

Hyperphosphorylation of tau is associated with conformational changes leading to tau misfolding and aggregation as the neurofibrillary tangles of Alzheimer's disease.[3,10] Aggregation of tau is mediated by the hydrophobic tubulin-binding domains (TBDs). The TBDs may be stabilized against aggregation by binding to microtubules, or via association with the N-terminus and C-terminus in a global hairpin conformation that masks the hydrophobic residues of the TBDs.[4,40] Phosphorylation or pseudophosphorylation induces structural changes that open this hairpin conformation, exposing the hydrophobic TBDs to promote aggregation, while OGlcNAcylation is protective against aggregation, potentially due to maintaining or stabilizing the global hairpin, though to date no structural data exist to suggest this latter possibility.[41] The importance of the N-terminus in protecting the TBDs from aggregation is emphasized by the ability of N-terminal tau peptides to inhibit tau aggregation, consistent with a critical role of the structure of the proline-rich linker between these domains in maintaining soluble tau.[42] Thus, changes in secondary structure in tau's proline-rich domain may mediate global changes in tau structure and function. Notably, phosphorylation at Ser-Pro and Thr-Pro sites within the proline-rich domain inhibits the ability of tau to promote tubulin polymerization.[5e] The most striking data herein are the high degree of order observed at phosphothreonine residues, with $^{3}J_{\alpha N}$ values that indicate very stable non-random coil conformation at these residues. Overall, these data indicate that phosphorylation of the tau proline-rich domain induces significant conformational changes that result in ordering of the proline-rich domain, particularly as observed by NMR in the dianionic state, whereas the effects of OGlcNAcylation are somewhat similar to the free Ser/Thr hydroxyls and specifically oppose the effects of phosphorylation, consistent with the observed effects of OGlcNAcylation in opposing tau aggregation.

Phosphorylation of threonine residues was found herein to induce greater structural changes than serine phosphorylation, although both phosphorylation events induced more ordered conformations, including induced PPII, restriction of ϕ, and slower amide exchange.[21a,31c,43] The greater structural change at Thr was due to a combination of both more disorder for nonphosphorylated Thr than Ser and more induced order for pThr than pSer, with particular conformational restriction of ϕ and evidence consistent with a phosphate-amide hydrogen bond. To identify a possible structural basis for these observations, phosphothreonine residues in several high resolution crystal structures (protein−protein interactions (see below) and globular proteins) were analyzed. The crystallographic data revealed a significant degree of conformational restriction in some phosphothreonine residues, consistent with the data herein. The conformation of phosphothreonine 197 in protein kinase A (pdb 1rdq, the highest resolution (1.26 Å) protein with pThr in the PDB) exhibits pThr in a PPII conformation (ϕ = −67°, ψ = +134°), χ_1 = −53° ($g-$), χ_2 = +119° (surprisingly, eclipsing C−H/O−P bonds), a hydrogen bond between the phosphate and the phosphothreonine amide, and close interaction between the n − 1 carbonyl (conjugated to the hydrogen-bonded pThr amide) and the pThr carbonyl (O−C distance 2.88 Å, substantially less than the 3.22 Å sum of van der Waals radii, as well as an O−C−O angle of 107°, similar to the Bürgi−Dunitz trajectory), as would be expected by a PPII-favoring $n \rightarrow \pi^*$ interaction (Figure 12).[44] Notably, Thr197 is a critical

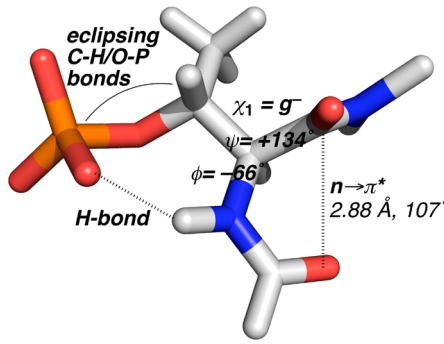

Figure 12. Structure of phosphothreonine residue 197 in protein kinase A (pdb 1rdq, 1.26 Å resolution).[44] A similar conformation of phosphothreonine (ϕ,ψ = −64°, +131°; $\chi_1 = g^-$; eclipsing C−H/O−P bonds (χ_2 = +118°); phosphate-amide hydrogen bond; n → π^* interaction) was observed in a tau peptide containing pThr231 bound to a monoclonal antibody (pdb 4glr), or of a pSer phosphopeptide bound to Pin1 (pdb 1f8a).[19b,46b] Hydrogens were added in Pymol.

and conserved residue in the activation loop of PKA and related protein kinases. Thr197 phosphorylation induces a substantial disorder-to-order transition in PKA and increase in PKA activity and stability, with Thr197 exhibiting no electron density in nonphosphorylated PKA.[45] The side chain conformational restriction observed crystallographically in phosphothreonine residues was also observed by NMR in Ac-KT(OPO_3^{2-})PP-NH_2, which exhibited $^{3}J_{H\alpha H\beta}$ = 9.5 Hz for phosphothreonine, near the maximum of the Karplus curve and indicating $\chi_1 \sim$ −60° ($g-$ rotamer) (compared to nonphosphorylated Thr

dx.doi.org/10.1021/ja407156m | J. Am. Chem. Soc. 2014, 136, 3803−3816

$^3J_{H\alpha H\beta}$ = 6.4 Hz, as expected for disorder; Figure S66, Supporting Information), as well as $^3J_{H\beta P}$ = 9 Hz, which is close to ideal for an eclipsing χ_2 C−H/O−P bond ($^3J_{H\beta P}$ = 9 Hz was also seen in tau$_{174-183}$; see Figures S20 and S77, Supporting Information). Collectively, the data observed herein across multiple phosphothreonine-containing peptides, including induction of polyproline helix by CD, small $^3J_{\alpha N}$ (= restricted ϕ) for phosphothreonine, large downfield changes in amide ^{1}H and ^{15}N chemical shifts, and slow amide hydrogen exchange, are consistent with this crystallographically observed conformation of phosphothreonine, suggesting a potentially general mode for conformational restriction by phosphothreonine residues in both disordered and globular proteins.

We previously observed that nature often employs the polyproline helix for phosphoprotein recognition by phosphoserine/phosphothreonine-binding domains, including binding of phosphopeptides in a polyproline helix by WW, FHA, Polo-box, and BRCT domains, though not by 14−3−3 domains.[7] In addition, recent analysis of phosphorylation sites in intrinsically disordered proteins suggests a greater propensity for PPII around phosphorylation sites.[37c] Serine and threonine have natively low PPII propensities, suggesting the possibility of phosphorylation-mediated switches to PPII.[7,15a] In proline-rich sequences, eukaryotic proteins also exhibit low frequencies of Asp and Glu residues, but high frequencies of Ser and Thr residues.[15a] These data suggest that phosphorylation can provide both conformational preference for PPII and anion specificity via electrostatics to protein-binding domains that recognize phosphorylated proteins via a polyproline helix conformation. Notably, tau phosphorylated at residue 231 is observed in a polyproline helix both when bound to the Pin1 WW domain (pdb 1i8h) and to an antiphosphotau antibody (pdb 4glr).[46] In this case, antibody recognition, which involves no inherent conformational bias in recognition epitopes, utilized PPII for high affinity (K_d = 1.1 nM) and high specificity (>500-fold specificity) recognition of the phosphorylated peptide over the nonphosphorylated peptide. In sum, these data suggest that polyproline helix provides the possibility of increased specificity and affinity in folding and recognition of phosphorylated Ser/Thr, over both nonphosphorylated or OGlcNAcylated Ser/Thr.

CONCLUSIONS

Phosphorylation and OGlcNAcylation are the most significant intracellular post-translational modifications of serine and threonine.[2] We found opposing structural effects of phosphorylation and OGlcNAcylation in proline-rich sequences, which are among the most common sequences in eukaryotes,[1] but similar effects of both modifications in opposing the unmodified hydroxyl in sequences with a nascent α-helix. These data provide a plausible structural basis for the observation that OGlcNAcylation of tau opposes neurofibrillary tangle formation, because of its confirmation of the disordered structure of sequences with unmodified serine and threonine residues, while phosphorylation is associated with neurofibrillary tangle formation, potentially because of a disorder to order transition that promotes opening of the global hairpin conformation of tau. More generally, these data provide a context for interpreting sequence-specific structural effects of these post-translational modifications, with broad potential application to understanding the intracellular effects of phosphorylation and OGlcNAcylation. Across all peptides, dianionic phosphoserine and dianionic phosphothreonine adopted ordered structures, including induction of polyproline helix. We found particular conformational restriction in phosphothreonine residues, with a highly ordered structure adopted. Notably, phosphoproteomics experiments have revealed that over 25% of phosphorylation sites are at Ser-Pro or Thr-Pro sequences, suggesting that the results observed herein in tau peptides and in proline-rich model peptides may have broad applicability in understanding the effects of phosphorylation on protein structure, particularly in regions of protein disorder.[37a]

EXPERIMENTAL SECTION

Peptide Synthesis and Characterization. Peptides were synthesized by Fmoc solid phase peptide synthesis. All peptides were acetylated at the N-terminus and contained C-terminal amides. Complete synthetic procedures and characterization data are in the Supporting Information.

Circular Dichroism. CD spectra were collected on a Jasco J-810 Spectropolarimeter in a 1 mm cell at 25 °C. Peptide concentrations were 15−400 μM in water containing 5 mM phosphate buffer (pH 8.0 or as indicated) and 25 mM KF. Data represent the average of at least three independent trials. Data were background corrected but were not smoothed. Error bars indicate standard error.

NMR Spectroscopy. NMR spectra of peptides were collected at 298 K on a Brüker AVC 600 MHz NMR spectrometer equipped with a triple resonance cryoprobe. ^{31}P NMR spectra were recorded on a Brüker DRX 400 MHz NMR spectrometer equipped with a BBO probe. Peptides were dissolved in buffer containing 5 mM phosphate (pH 4.0, 6.5, 7.2, or 8.0) with 25 mM NaCl, 100 μM TSP, and 90% H_2O/10% D_2O. $^3J_{\alpha N}$ and $^3J_{HP}$ were determined directly from the 1-D ^{1}H NMR spectra and proton-coupled ^{31}P NMR spectra, respectively.

ASSOCIATED CONTENT

Supporting Information

Synthesis of protected Fmoc OGlcNAcylated amino acids, peptide synthesis and characterization, CD data on model peptides, and full NMR spectroscopy data. This material is available free of charge via the Internet at http://pubs.acs.org.

AUTHOR INFORMATION

Corresponding Author

zondlo@udel.edu

Author Contributions

†M.A. Brister and A. K. Pandey contributed equally to this work.

Notes

The authors declare no competing financial interest.

ACKNOWLEDGMENTS

We thank the Alzheimer's Association (NIRG-06-14403), NIH (GM93225), HHMI (undergraduate research fellowships for M.A.B. and A.A.B.), and the University of Delaware for funding. We thank Alaina Brown, Ben Liechty, and Krista Thomas for preliminary structural studies on phosphorylated peptides.

REFERENCES

(1) Rubin, G. M.; Yandell, M. D.; Wortman, J. R.; Miklos, G. L. G.; Nelson, C. R.; Hariharan, I. K.; Fortini, M. E.; Li, P. W.; Apweiler, R.; Fleischmann, W.; Cherry, J. M.; Henikoff, S.; Skupski, M. P.; Misra, S.; Ashburner, M.; Birney, E.; Boguski, M. S.; Brody, T.; Brokstein, P.; Celniker, S. E.; Chervitz, S. A.; Coates, D.; Cravchik, A.; Gabrielian, A.; Galle, R. F.; Gelbart, W. M.; George, R. A.; Goldstein, L. S. B.; Gong, F. C.; Guan, P.; Harris, N. L.; Hay, B. A.; Hoskins, R. A.; Li, J. Y.; Li, Z. Y.; Hynes, R. O.; Jones, S. J. M.; Kuehl, P. M.; Lemaitre, B.; Littleton,

J. T.; Morrison, D. K.; Mungall, C.; O'Farrell, P. H.; Pickeral, O. K.; Shue, C.; Vosshall, L. B.; Zhang, J.; Zhao, Q.; Zheng, X. Q. H.; Zhong, F.; Zhong, W. Y.; Gibbs, R.; Venter, J. C.; Adams, M. D.; Lewis, S. *Science* **2000**, *287*, 2204−2215.
(2) Hart, G. W.; Slawson, C.; Ramirez-Correa, G.; Lagerlof, O. *Annu. Rev. Biochem.* **2011**, *80*, 825−858.
(3) (a) Buée, L.; Bussière, T.; Buée-Scherrer, V.; Delacourte, A.; Hof, P. R. *Brain Res. Rev.* **2000**, *33*, 95−130. (b) Hernandez, F.; Avila, J. *Cell. Mol. Life Sci.* **2007**, *64*, 2219−2233.
(4) Jeganathan, S.; von Bergen, M.; Brutlach, H.; Steinhoff, H.-J.; Mandelkow, E. *Biochemistry* **2006**, *45*, 2283−2293.
(5) (a) Lippens, G.; Wieruszeski, J.-M.; Leroy, A.; Smet, C.; Sillen, A.; Buée, L.; Landrieu, I. *ChemBioChem* **2004**, *5*, 73−78. (b) Smet, C.; Leroy, A.; Sillen, A.; Wieruszeski, J.-M.; Landrieu, I.; Lippens, G. *ChemBioChem* **2004**, *5*, 1639−1646. (c) Landrieu, I.; Lacosse, L.; Leroy, A.; Wieruszeski, J. M.; Trivelli, X.; Sillen, A.; Sibille, N.; Schwalbe, H.; Saxena, K.; Langer, T.; Lippens, G. *J. Am. Chem. Soc.* **2006**, *128*, 3575−3583. (d) Smet-Nocca, C.; Broncel, M.; Wieruszeski, J. M.; Tokarski, C.; Hanoulle, X.; Leroy, A.; Landrieu, I.; Rolando, C.; Lippens, G.; Hackenberger, C. P. R. *Mol. BioSyst.* **2011**, *7*, 1420−1429. (e) Sibille, N.; Huvent, I.; Fauquant, C.; Verdegem, D.; Amniai, L.; Leroy, A.; Wieruszeski, J. M.; Lippens, G.; Landrieu, I. *Proteins* **2012**, *80*, 454−462. (f) Theillet, F. X.; Smet-Nocca, C.; Liokatis, S.; Thongwichian, R.; Kosten, J.; Yoon, M. K.; Kriwacki, R. W.; Landrieu, I.; Lippens, G.; Selenko, P. *J. Biomol. NMR* **2012**, *54*, 217−236.
(6) Broncel, M.; Krause, E.; Schwarzer, D.; Hackenberger, C. P. R. *Chem.—Eur. J.* **2012**, *18*, 2488−2492.
(7) Bielska, A. A.; Zondlo, N. J. *Biochemistry* **2006**, *45*, 5527−5537.
(8) Liu, F.; Iqbal, K.; Grundke-Iqbal, I.; Hart, G. W.; Gong, C. X. *Proc. Natl. Acad. Sci. U. S. A.* **2004**, *101*, 10804−10809.
(9) Yuzwa, S. A.; Shan, X. Y.; Macauley, M. S.; Clark, T.; Skorobogatko, Y.; Vosseller, K.; Vocadlo, D. J. *Nat. Chem. Biol.* **2012**, *8*, 393−399.
(10) Wang, J. Z.; Xia, Y. Y.; Grundke-Iqbal, I.; Iqbal, K. *J. Alzheimer's Dis.* **2013**, *33*, S123−S139.
(11) Arsequell, G.; Krippner, L.; Dwek, R. A.; Wong, S. Y. C. *Chem. Commun.* **1994**, 2383−2384.
(12) Sjölin, P.; Elofsson, M.; Kihlberg, J. *J. Org. Chem.* **1996**, *61*, 560−565.
(13) (a) Thomas, K. M.; Naduthambi, D.; Tririya, G.; Zondlo, N. J. *Org. Lett.* **2005**, *7*, 2397−2400. (b) Pandey, A. K.; Naduthambi, D.; Thomas, K. M.; Zondlo, N. J. *J. Am. Chem. Soc.* **2013**, *135*, 4333−4363.
(14) (a) Williamson, M. P. *Biochem. J.* **1994**, *297*, 249−260. (b) Adzhubei, A. A.; Sternberg, M. J. E.; Makarov, A. A. *J. Mol. Biol.* **2013**, *425*, 2100−2132.
(15) (a) Brown, A. M.; Zondlo, N. J. *Biochemistry* **2012**, *51*, 5041−5051. (b) Kelly, M. A.; Chellgren, B. W.; Rucker, A. L.; Troutman, J. M.; Fried, M. G.; Miller, A. F.; Creamer, T. P. *Biochemistry* **2001**, *40*, 14376−14383. (c) Rucker, A. L.; Pager, C. T.; Campbell, M. N.; Qualls, J. E.; Creamer, T. P. *Proteins* **2003**, *53*, 68−75. (d) Sreerama, N.; Woody, R. W. *Biochemistry* **1994**, *33*, 10022−10025. (e) Woody, R. W. *J. Am. Chem. Soc.* **2009**, *131*, 8234−8245.
(16) (a) Shi, Z. S.; Olson, C. A.; Rose, G. D.; Baldwin, R. L.; Kallenbach, N. R. *Proc. Natl. Acad. Sci. U. S. A.* **2002**, *99*, 9190−9195. (b) Ding, L.; Chen, K.; Santini, P. A.; Shi, Z.; Kallenbach, N. R. *J. Am. Chem. Soc.* **2003**, *125*, 8092−8093. (c) Chen, K.; Liu, Z. G.; Zhou, C. H.; Shi, Z. S.; Kallenbach, N. R. *J. Am. Chem. Soc.* **2005**, *127*, 10146−10147. (d) Shi, Z.; Chen, K.; Liu, Z.; Ng, A.; Bracken, W. C.; Kallenbach, N. R. *Proc. Natl. Acad. Sci. U. S. A.* **2005**, *102*, 17964−17968. (e) Lam, S. L.; Hsu, V. L. *Biopolymers* **2003**, *69*, 270−281.
(17) (a) Dunbrack, R. L., Jr.; Karplus, M. *J. Mol. Biol.* **1993**, *230*, 543−574. (b) Lovell, S. C.; Word, J. M.; Richardson, J. S.; Richardson, D. C. *Proteins* **2000**, *40*, 389−408. (c) Vijayakumar, M.; Qian, H.; Zhou, H. X. *Proteins* **1999**, *34*, 497−507. (d) Eswar, N.; Ramakrishnan, C. *Protein Eng.* **2000**, *13*, 227−238.
(18) Mukrasch, M. D.; Bibow, S.; Korukottu, J.; Jeganathan, S.; Biernat, J.; Griesinger, C.; Mandelkow, E.; Zweckstetter, M. *PLoS Biol.* **2009**, *7*, 399−414.
(19) (a) Simanek, E. E.; Huang, D. H.; Pasternack, L.; Machajewski, T. D.; Seitz, O.; Millar, D. S.; Dyson, H. J.; Wong, C. H. *J. Am. Chem. Soc.* **1998**, *120*, 11567−11575. (b) Verdecia, M. A.; Bowman, M. E.; Lu, K. P.; Hunter, T.; Noel, J. P. *Nat. Struct. Biol.* **2000**, *7*, 639−643.
(20) (a) Ruiz-Carrillo, D.; Koch, B.; Parthier, C.; Wermann, M.; Dambe, T.; Buchholz, M.; Ludwig, H. H.; Heiser, U.; Rahfeld, J. U.; Stubbs, M. T.; Schilling, S.; Demuth, H. U. *Biochemistry* **2011**, *50*, 6280−6288. (b) Patino, E.; Kotzsch, A.; Saremba, S.; Nickel, J.; Schmitz, W.; Sebald, W.; Mueller, T. D. *Structure* **2011**, *19*, 1864−1875.
(21) (a) Szilak, L.; Moitra, J.; Krylov, D.; Vinson, C. *Nat. Struct. Biol.* **1997**, *4*, 112−114. (b) Andrew, C. D.; Warwicker, J.; Jones, G. R.; Doig, A. J. *Biochemistry* **2002**, *41*, 1897−1905.
(22) Wishart, D. S.; Sykes, B. D. *J. Biomol. NMR* **1994**, *4*, 171−180.
(23) (a) Serrano, L.; Fersht, A. R. *Nature* **1989**, *342*, 296−299. (b) Doig, A. J.; Baldwin, R. L. *Protein Sci.* **1995**, *4*, 1325−1336. (c) Aurora, R.; Rose, G. D. *Protein Sci.* **1998**, *7*, 21−38. (d) MacArthur, M. W.; Thornton, J. M. *J. Mol. Biol.* **1991**, *218*, 397−412.
(24) Cammers-Goodwin, A.; Allen, T. J.; Oslick, S. L.; McClure, K. F.; Lee, J. H.; Kemp, D. S. *J. Am. Chem. Soc.* **1996**, *118*, 3082−3090.
(25) Bibow, S.; Ozenne, V.; Biernat, J.; Blackledge, M.; Mandelkow, E.; Zweckstetter, M. *J. Am. Chem. Soc.* **2011**, *133*, 15842−15845.
(26) (a) Cochran, D. A. E.; Doig, A. J. *Protein Sci.* **2001**, *10*, 1305−1311. (b) Cochran, D. A. E.; Penel, S.; Doig, A. J. *Protein Sci.* **2001**, *10*, 463−470.
(27) (a) O'Neil, K. T.; Degrado, W. F. *Science* **1990**, *250*, 646−651. (b) Blaber, M.; Zhang, X. J.; Matthews, B. W. *Science* **1993**, *260*, 1637−1640. (c) Zondlo, S. C.; Lee, A. E.; Zondlo, N. J. *Biochemistry* **2006**, *45*, 11945−11957.
(28) Mukrasch, M. D.; von Bergen, M.; Biernat, J.; Fischer, D.; Griesinger, C.; Mandelkow, E.; Zweckstetter, M. *J. Biol. Chem.* **2007**, *282*, 12230−12239.
(29) (a) Radhakrishnan, I.; Pérez-Alvarado, G. C.; Dyson, H. J.; Wright, P. E. *FEBS Lett.* **1998**, *430*, 317−322. (b) Tholey, A.; Lindemann, A.; Kinzel, V.; Reed, J. *Biophys. J.* **1999**, *76*, 76−87. (c) Bienkiewicz, E. A.; Lumb, K. J. *J. Biomol. NMR* **1999**, *15*, 203−206. (d) Wong, S. E.; Bernacki, K.; Jacobson, M. *J. Phys. Chem. B* **2005**, *109*, 5249−5258. (e) Lee, K. K.; Joo, C.; Yang, S.; Han, H.; Cho, M. *J. Chem. Phys.* **2007**, 126. (f) Kim, S. Y.; Jung, Y.; Hwang, G. S.; Han, H.; Cho, M. *Proteins* **2011**, *79*, 3155−3165.
(30) Vuister, G. W.; Bax, A. *J. Am. Chem. Soc.* **1993**, *115*, 7772−7777.
(31) (a) Hol, W. G. J.; Vanduijnen, P. T.; Berendsen, H. J. C. *Nature* **1978**, *273*, 443−446. (b) Radhakrishnan, I.; Perez-Alvarado, G. C.; Parker, D.; Dyson, H. J.; Montminy, M.; Wright, P. E. *Cell* **1997**, *91*, 741−752. (c) Szilak, L.; Moitra, J.; Vinson, C. *Protein Sci.* **1997**, *6*, 1273−1283. (d) Signarvic, R. S.; DeGrado, W. F. *J. Mol. Biol.* **2003**, *334*, 1−12. (e) Errington, N.; Doig, A. J. *Biochemistry* **2005**, *44*, 7553−7558. (f) Balakrishnan, S.; Zondlo, N. J. *J. Am. Chem. Soc.* **2006**, *128*, 5590−5591. (g) Zondlo, S. C.; Gao, F.; Zondlo, N. J. *J. Am. Chem. Soc.* **2010**, *132*, 5619−5621. (h) Smart, J. L.; McCammon, J. A. *Biopolymers* **1999**, *49*, 225−233.
(32) See the Supporting Information for details.
(33) Creamer, T. P. *Proteins* **1998**, *33*, 218−226.
(34) (a) Bretscher, L. E.; Jenkins, C. L.; Taylor, K. M.; DeRider, M. L.; Raines, R. T. *J. Am. Chem. Soc.* **2001**, *123*, 777−778. (b) Hinderaker, M. P.; Raines, R. T. *Protein Sci.* **2003**, *12*, 1188−1194. (c) Hodges, J. A.; Raines, R. T. *Org. Lett.* **2006**, *8*, 4695−4697. (d) Bartlett, G. J.; Choudhary, A.; Raines, R. T.; Woolfson, D. N. *Nat. Chem. Biol.* **2010**, *6*, 615−620. (e) Choudhary, A.; Fry, C. G.; Kamer, K. J.; Raines, R. T. *Chem. Commun.* **2013**, *49*, 8166−8168. (f) Newberry, R. W.; VanVeller, B.; Guzei, I. A.; Raines, R. T. *J. Am. Chem. Soc.* **2013**, *135*, 7843−7846. (g) Zondlo, N. J. *Nat. Chem. Biol.* **2010**, *6*, 567−568.
(35) Du, J.-T.; Li, Y.-M.; Wei, W.; Wu, G.-S.; Zhao, Y.-F.; Kanazawa, K.; Nemoto, T.; Nakanishi, H. *J. Am. Chem. Soc.* **2005**, *127*, 16350−16351.
(36) Horng, J. C.; Raines, R. T. *Protein Sci.* **2006**, *15*, 74−83.
(37) (a) Ubersax, J. A.; Ferrell, J. E. *Nat. Rev. Mol. Cell Biol.* **2007**, *8*, 530−541. (b) Chen, S.; Chen, F.; Li, W. *Mol. Biol. Evol.* **2010**, *27*,

2548−2554. (c) Elam, W. A.; Schrank, T. P.; Campagnolo, A. J.; Hilser, V. J. *Protein Sci.* **2013**, *22*, 405−417.
(38) Opposing effects of phosphorylation versus OGlcNAcylation on turn formation in the estrogen receptor at Ser16: (a) Chen, Y. X.; Du, J. T.; Zhou, L. X.; Liu, X. H.; Zhao, Y. F.; Nakanishi, H.; Li, Y. M. *Chem. Biol.* **2006**, *13*, 937−944. Opposing structural effects of phosphorylation and OGlcNAcylation in different residues in β-hairpin peptides: (b) Laughrey, Z. R.; Kiehna, S. E.; Riemen, A. J.; Waters, M. L. *J. Am. Chem. Soc.* **2008**, *130*, 14625−14633. (c) Riemen, A. J.; Waters, M. L. *J. Am. Chem. Soc.* **2009**, *131*, 14081−14087. (d) Riemen, A. J.; Waters, M. L. *J. Am. Chem. Soc.* **2010**, *132*, 9007−9013. (e) Riemen, A. J.; Waters, M. L. *Org. Biomol. Chem.* **2010**, *8*, 5411−5417. Examination of phosphorylation versus *O*-galactose modification in α-helices: (f) Broncel, M.; Falenski, J. A.; Wagner, S. C.; Hackenberger, C. P. R.; Koksch, B. *Chem.—Eur. J.* **2010**, *16*, 7881−7888. The effects of Thr phosphorylation (at pH 5.2) versus OGlcNAcylation were examined in the loop of a designed α-helical hairpin. While neither post-translational modification significantly affected the thermal stability of the helical hairpin, both post-translational modifications dramatically and differentially affected its rate of aggregation: (g) Liang, F.-C.; Chen, R. P.-Y.; Lin, C.-C.; Huang, K.-T.; Chan, S. I. *Biochem. Biophys. Res. Commun.* **2006**, *342*, 482−488. (h) Chen, P.-Y.; Lin, C.-C.; Chang, Y.-T.; Lin, S.-C.; Chan, S. I. *Proc. Natl. Acad. Sci. U. S. A.* **2002**, *99*, 13633−13638.
(39) Iakoucheva, L. M.; Radivojac, P.; Brown, C. J.; O'Connor, T. R.; Sikes, J. G.; Obradovic, Z.; Dunker, A. K. *Nucleic Acids Res.* **2004**, *32*, 1037−1049.
(40) Elbaum-Garfinkle, S.; Rhoades, E. *J. Am. Chem. Soc.* **2012**, *134*, 16607−16613.
(41) (a) Jeganathan, S.; Hascher, A.; Chinnathambi, S.; Biernat, J.; Mandelkow, E. M.; Mandelkow, E. *J. Biol. Chem.* **2008**, *283*, 32066−32076. (b) Combs, B.; Voss, K.; Gamblin, T. C. *Biochemistry* **2011**, *50*, 9446−9456. (c) Daly, N. L.; Hoffmann, R.; Otvos, L., Jr.; Craik, D. J. *Biochemistry* **2000**, *39*, 9039−9046.
(42) Horowitz, P. M.; LaPointe, N.; Guillozet-Bongaarts, A. L.; Berry, R. W.; Binder, L. I. *Biochemistry* **2006**, *45*, 12859−12866.
(43) Examples of structural differences of Ser versus Thr phosphorylation in α-helices: refs 21a, 31c. Examples of differential structural effects of Ser versus Thr glycosylation: (a) Tachibana, Y.; Fletcher, G. L.; Fujitani, N.; Tsuda, S.; Monde, K.; Nishimura, S. I. *Angew. Chem., Int. Ed.* **2004**, *43*, 856−862. (b) Corzana, F.; Busto, J. H.; Jimenez-Oses, G.; de Luis, M. G.; Asensio, J. L.; Jimenez-Barbero, J.; Peregrina, J. M.; Avenoza, A. *J. Am. Chem. Soc.* **2007**, *129*, 9458−9467. (c) Fernandez-Tejada, A.; Corzana, F.; Busto, J. H.; Jimenez-Oses, G.; Jimenez-Barbero, J.; Avenoza, A.; Peregrina, J. M. *Chem.—Eur. J.* **2009**, *15*, 7297−7301.
(44) Yang, J.; Ten Eyck, L. F.; Xuong, N.-H.; Taylor, S. S. *J. Mol. Biol.* **2004**, *336*, 473−487.
(45) (a) Steichen, J. M.; Iyer, G. H.; Li, S.; Saldanha, S. A.; Deal, M. S.; Woods, V. L.; Taylor, S. S. *J. Biol. Chem.* **2010**, *285*, 3825−3832. (b) Steichen, J. M.; Kuchinskas, M.; Keshwani, M. M.; Yang, J.; Adams, J. A.; Taylor, S. S. *J. Biol. Chem.* **2012**, *287*, 14672−14680.
(46) (a) Wintjens, R.; Wieruszeski, J.-M.; Drobecq, H.; Rousselot-Pailley, P.; Buée, L.; Lippens, G.; Landrieu, I. *J. Biol. Chem.* **2001**, *276*, 25150−25156. (b) Shih, H. H.; Tu, C.; Cao, W.; Klein, A.; Ramsey, R.; Fennell, B. J.; Lambert, M.; Shúilleabháin, D. N.; Autin, B.; Kouranova, E.; Laxmanan, S.; Braithwaite, S.; Wu, L.; Ait-Zahra, M.; Milici, A. J.; Dumin, J. A.; LaVallie, E. R.; Arai, M.; Corcoran, C.; Paulsen, J. E.; Gill, D.; Cunningham, O.; Bard, J.; Mosyak, L.; Finlay, W. J. J. *J. Biol. Chem.* **2012**, *287*, 44425−44434.